HHS Public Access

Author manuscript

ACS Appl Mater Interfaces. Author manuscript; available in PMC 2019 September 26.

Published in final edited form as:

ACS Appl Mater Interfaces. 2018 September 26; 10(38): 32782–32791. doi:10.1021/acsami.8b07573.

Membrane-less compartmentalization facilitates enzymatic cascade reactions and reduces substrate inhibition.

Taisuke Kojima[1] and **Shuichi Takayama**[1,2,*]

[1]The Wallace H Coulter Department of Biomedical Engineering, Georgia Institute of Technology and Emory School of Medicine, Atlanta, GA 30332 USA

[2]The Parker H Petit Institute for Bioengineering and Bioscience, Georgia Institute of Technology, Atlanta GA 30332 USA

Abstract

Living cells possess membraneless-organelles formed by liquid-liquid phase separation. With the aim of better understanding the general functions of membrane-less microcompartments, this paper constructs acellular multi-compartment reaction systems using an aqueous multi-phase system. Membrane-less coacervate droplets are placed within a molecularly crowded environment where a larger dextran (DEX) droplet is submerged in a polyethylene glycol (PEG) solution. The coacervate droplets are capable of sequestering reagents and enzymes with a long retention time, and demonstrate multi-step cascading reactions through the liquid-liquid interfaces. The ability to change phase dynamics is also demonstrated through salt-mediated dissolution of coacervate droplets, which leads to release and mixing of separately sequestered reagents and enzymes. Finally, as phase-separated materials in membraneless organelles are often substrates and substrate analogues for the enzymes sequestered or excluded in the organelles, this paper explores the interaction between DEX and dextranase, an enzyme that hydrolyzes DEX. Results revealed that dextranase suffers from substrate inhibition when partitioned directly in a DEX phase but that this inhibition can be mitigated and reactions greatly accelerated by compartmentalization of dextranase inside a coacervate droplet that is adjacent to, but phase-separated from, the DEX phase. The insight that compartmentalization of enzymes can accelerate reactions by mitigating substrate inhibition is particularly novel and is an example where artificial membrane-less organelle-like systems may provide new insights into physiological cell functions.

[*]To whom correspondence should be addressed: Prof. Shuichi Takayama, EBB Building, 950 Atlantic Drive NW, Georgia Institute of Technology, GA, USA 30332, takayama@bme.gatech.edu.

Supporting Information Available:

This material is available free of charge via the Internet at http://pubs.acs.org. The supporting information includes the zeta potential and partition coefficient values of the enzymes, wetting behavior of the ATP-PDDA coacervates upon suspension and resuspension, coacervate encapsulation of food colorings after centrifugation, time-lapse retention of the coacervates containing food colorings in the DEX-PEG ATPS, sensitivity of the coacervates in the ATPS upon pH and ionic strength changes, selective dissociation of the coacervates in the ATPS by NaCl addition, fluorometric GOx-HRP-mediated cascade reactions, time-lapse GOx partitioning to the ATP-PDDA coacervate phase in the DEXPEG system, different size ATP-PDDA coacervates after the DAB-catalyzing cascade reaction, and the relative viscosity measurement of the DEX and coacervate solutions.

The authors declare no competing financial interests.

Graphical abstract

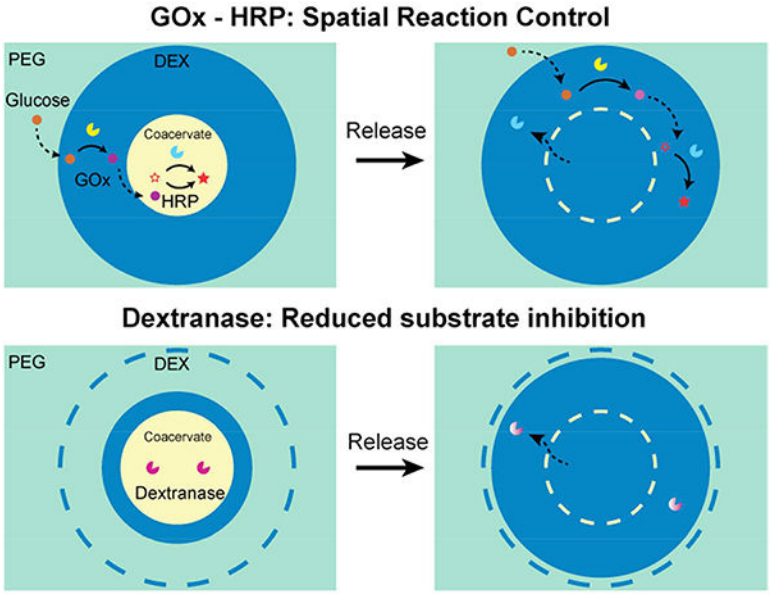

Keywords

Aqueous Two Phase System; Complex Coacervation; Liquid-Liquid Phase Separation; Compartmentalization; Membrane-less Organelle

1. Introduction

Intracellular subcompartments regulate biological events and facilitate biochemical reactions through isolation, localization, and subsequent release of biomolecules facilitated by compartmentalization. Reaction networks in engineered microcompartments that mimic cellular organelles can enhance understanding of intracellular processes, allow added control in synthetic biology applications, and provide insights into the origin of life.[1–4] Most such systems, however, mimic conventional membrane-bounded organelles such as the nucleus and mitochondria. Recently, there have been both multiple discoveries of and increased appreciation for membraneless compartmentalization through liquid-liquid phase separation (LLPS) in cells.[5–7] Cells seemingly utilize molecular crowding to spatiotemporally regulate LLPS.[8–10] The properties and biological functions of these membrane-less organelles are much less understood compared to their membrane-bounded counterparts. Some functions of membrane-less compartmentalization include concentration and storage of active biomolecules,[11] regulation of biochemical reactions and kinetics,[12, 13] mediation of stress,[14–16] and potential protection from toxic macromolecules.[17] However, the link between the underlying mechanisms and functions, particularly how membrane-less compartmentalization regulates enzymatic reactions and kinetics, is still elusive.

Here we report an LLPS-based multi-compartment system in a molecularly crowded environment constructed through the combination of complex coacervation of adenosine triphosphate (ATP) and poly(diallyldimethylammonium chloride) (PDDA),[18, 19] and an

aqueous two-phase system (ATPS) comprising dextran (DEX) and polyethylene glycol (PEG)[20–22] in order to explore the capability of membrane-less compartments to sequester reagents, regulate cascading reactions, and accelerate enzymatic reactions. In particular, we propose a new mechanism of reaction acceleration by membrane-less compartmentalization that is based on the reduction of substrate inhibition. We show that substrate inhibition occurs for dextranase in highly concentrated DEX macromolecules, whereas it can be circumvented by sequestration of the enzyme in membrane-less compartments that are adjacent to, but phase separated from, the DEX phase.

While often overlooked, substrate inhibition in biochemical reactions is prevalent in living systems.[23] For example, alchohol deoxygenase and tyrosine hydroxylase in the central nervous system, and phosphofructokinase and deoxyribonucleic acid (DNA) methyltransferase with nucleic acid substrates in the nucleus both show strong substrate / substrate analogue inhibition. Although our example using DEX and endo-dextranase is a specialized example, it is noted that membraneless organelles in cells can also sequester or exclude the enzymes that use the phase forming materials as substrates. Such a prominent example is the nucleolus[24] that forms a multi-phase membraneless organelle comprised of ribonucleic acid (RNA) and their binding proteins; and compartmentalizes ribosomal DNA and RNA, RNA polymerase (RNAP), and the preribosomal particles in dedicated domains within the organelle to promote transcription and translation.[25] Our system recapitulates such characteristics and serves as a model platform to explore organelle function.

In this work, we first evaluate the structural stability and molecular retention of the ATPPDDA coacervates in the DEX-PEG system and demonstrate the ionic strength-mediated release of coacervate-encapsulated substances into the DEX phase. Next we perform a two-enzyme cascade reaction that occurs with substrate transport across compartments, and compare the reaction between compartmentalized and released enzyme-substrate sets. The platform is further illustrated in a multiple substrate format to generate different colorimetric products in different compartments in a spatiotemporally controlled manner. Finally, we disintegrate compartmentalization by enzymatic degradation of the DEX phase and assess the effect of compartmentalization, including its ability to mitigate substrate inhibition.

2. Materials and Methods

All reagents were purchased through commercially available sources: dextran (DEX: Mw 500,000), polyethylene glycol (PEG: Mw 35,000), horseradish peroxidase (HRP: 150 units mg^{-1}), glucose oxidase (GOx: 15 units mg^{-1}), dextranase (17.5 and 175 units mg^{-1}), fluorescein isothiocyanate (FITC), rhodamine B isothiocyanate (RITC), ampliflu™ red, 2,2’-azino-bis(3-ethylbenzothiazoline-6-sulfonic acid) diammonium salt (ABTS), 3,3’-diaminobenzidine (DAB), o-phenylenediamine (oPD), 2-(N-morpholino)ethanesulfonic acid (MES) monohydrate, 3-morpholinopropane-1-sulfonic acid (MOPS), sodium hydroxide (6 M NaOH), hydrochloric acid (1M HCl), and Pur-A-Lyzer Maxi dialysis kit (Mw cutoff 12,000) were from Millipore-Sigma. FITC-DEX (Mw 500,000) was from TdB Consultancy AB. Food colorings (blue, green, red, and yellow) were from ESCO Foods. 35 mm glass-bottom dishes (No.0) were from MatTek Corp. Flat-bottom 24-well plates were from

Corning. Fluorescent labelling of enzymes and characterization of ATP-PDDA coacervates were conducted using a previously reported protocol[26] and described in the supporting information.

2.1 Preparation of ATP-PDDA coacervates and a DEX-PEG ATPS

MES buffer (20 mM, pH 6.0), ATP (50 mM, MES, pH 6.0), PDDA (50 mM, MES, pH 6.0), 500 kg mol^{-1} DEX (10 % w/w, MES, pH 6.0), and 35 kg mol^{-1} PEG (10 % w/w, MES, pH 6.0) solutions were prepared and filtrated using a 0.45 μm syringe filter (Puradisc™, Whatman). Given high resistance to wetting on a substrate,[27] ATP-PDDA coacervates isolated in resuspension were utilized (Figure S1). ATP, PDDA, and loading materials were mixed and centrifuged at 5,000 rpm for 5 min. After the supernatant was removed, the remaining coacervate-rich pellet was stored at 4 °C and used within the same day of preparation. The surface potential and molecular composition of the ATP-PDDA coacervates were consistent with previously reported values (Ref 18 and 26) and summarized in Table S1. An ATPS comprising 10 % w/w DEX and 10 % w/w PEG above the critical concentration[28] was used.

2.2 Confocal imaging of the ATP-PDDA coacervate in the DEX-PEG ATPS

Rhodamine B (final concentration of 1 μM) was premixed in the preparation of coacervates. 50 μL of a DEX droplet containing 1 mg mL^{-1} FITC-DEX was placed on a glass-bottom dish and 0.5 μL of the coacervate was spotted in the DEX droplet. 500 μL of a PEG solution was gently added to the dish to form a three-phase system. Fluorescent z-stack images were collected (Nikon-A1, Nikon) and processed by ImageJ (NIH).

2.3 Molecular Stability of the ATP-PDDA coacervate

1 μL of the coacervate was spotted in 50 μL of either MES buffer or the DEX solutions. The supernatant was collected at specific time points (t = 0 – 24 hours) and measured by a UV-VIS spectroscopy (NanoVue, Nanodrop). The subtracted absorbance ($A^{260\ nm}$ - $A^{320\ nm}$) was utilized to calculate the released ATP concentration in the supernatant using the extinction coefficient of ATP (15.4 mM^{-1} cm^{-1}). The total ATP concentration was obtained by complete dissociation of the coacervate in the presence of 500 mM NaCl. The ratio (mol %) of the released ATP to the total ATP was averaged with three replicates and expressed as mean with standard deviation.

2.4 Patterning and degradation of the ATP-PDDA coacervates in the DEX-PEG ATPS

1000-fold diluted food colorings (red, yellow, green, and blue) were premixed during coacervation. 50 μL of a DEX solution was dispensed on a plastic plate (24-well plate, Corning Coaster) and 0.5 μL of a coacervate pellet was spotted in the DEX droplet. 500 μL of PEG or PEG-NaCl solutions (200 mM NaCl) was added to the DEX solution for retention or release of food colorings, respectively. Time-lapse images were collected with a stereoscope (C-DSD115, Nikon) at t = 0, 24, and 72 hrs for the retention measurement and at t = 0 through 35 min and t = 1200 min for the release measurement. Note that food colorings comprise a combination of dyes such as brilliant blue, allura red, and tartrazine yellow. Each food coloring shows different partitioning behavior (Figure S2).

2.5 Compartentalized enzymatic cascade reactions across the coacervate, DEX, and PEG phases.

HRP (final concentration 0.1 mg mL^{-1}, MES, pH 6.0) and ABTS (final concentration 1 mg mL^{-1}, MES, pH 6.0), DAB (final concentration 1 mg mL^{-1}, DMSO), oPD (final concentration 1 mg mL^{-1}, DMSO), or Ampliflu™ Red (final concentration 1 mg mL^{-1}, DMSO) were premixedduring coacervation. 50 μL of a DEX solution containing GOx (final concentration 0.1 mg mL^{-1}, MES, pH 6.0) was dispensed on the plastic plate and 0.5 μL of the coacervates were spotted in the DEX droplet. 500 μL of a PEG solution was gently added to the dish. A glucose solution (final concentration 1 mM, MES, pH 6.0) was added to the PEG solution at 24 °C and images were taken using the stereoscope or an epifluorescent microscope (TE-300, Nikon).

2.6 Quantification of the enzymatic cascade reactions with compartmentalized and released HRP.

HRP (final concentration 0.1 mg mL^{-1}, MES, pH 6.0) and DAB (final concentration 1 mg mL^{-1}, DMSO) or oPD (final concentration 1 mg mL^{-1}, DMSO) were premixed during coacervation. 1,3 μL of the coacervate pellet was spotted into 50 μL of a DEX solution containing 0.1 mg mL^{-1} GOx on a 24-well plastic plate. 200 μL of a PEG solution (± 200 mM NaCl) was gently added and set for 30 min. For comparison of the droplet size, 1, 3, or 9 μL of the coacervate droplet encapuslating the same amount of HRP was used. A glucose solution (final concentration 1 mM) was added to each well except blank conditions in the absence of glucose, and absorbance changes for DAB and oPD were monitored (Synergy™ H4 Hybrid Microplate Reader, BioTek) at 471 nm and 492 nm, respectively, every 3 min for 90 min at 24 °C. The final absorbance values were averaged with three replicates and expressed as mean with standard deviation.

2.7 Degradation of DEX by compartmentalized or released dextranase

Dextranase (final concentration 0.1 mg mL^{-1}, MES, pH 6.0) was premixed in the coacervates. 10 μL of a DEX solution containing 1 μg mL^{-1} FITC-DEX was added to each well in a 24-well plate. 0.5 μL of dextranase-laden coacervates were dispensed into the DEX droplet. 500 μL of a PEG solution (± 150 mM NaCl, MES, pH 6.0) was added to each well. 0.5 μL of ATP-PDDA coacervates alone was used as a blank condition. Time-lapse images were taken at 24 °C by the epifluorescent microscope. The surface area of the DEX droplet was analyzed by ImageJ. The area values were averaged with three replicates and expressed as mean with standard deviation.

2.8 Bulk dextranase assay with compartmentalized or released dextranase

The detailed protocol is described in the supporting information. Briefly, dextranase degrades dextran that produces terminal isomaltose groups that convert a color reagent (3,5-dinitrosalicylic acid) into a colorimetric product (3-amino-5-nitrosalicylic acid: λ^{abs} = 540 nm) under basic conditions. A calibration curve was determined using maltose and 500 kg mol^{-1} DEX (0.5, 1, 2, 3, 4, 8, 10, and 20 % w/w, 0.1 M KH_2PO_4, pH 6.0) was used for the assay. The mass of dextranase was set to be around 2 μg per assay. The specific activity of dextranase was defined as unit mg^{-1} where one unit liberate one micromole of isomaltose

per min at pH 6.0 at 24 °C. The values were averaged with three replicates and expressed as mean with standard deviation.

2.9 Statistical analysis

ANOVA tests were performed using a commercially-available software package (SigmaStat 3.5, Systat Software Inc.), using Student's t-test or Tukey's test for post-hoc pairwise comparisons.

3. Results and Discussion

Membrane-less compartmentalization using ATP-PDDA coacervates in a DEX-PEG ATPS

The proximity of most membrane-less organelles to critical points for phase transition along with their relatively open nature of compartmentalization allows dynamic exchange of molecules and phase transition triggered by relatively small changes in the external microenvironment.[29, 30] In this paper, we first validated the integration of complex coacervation in an ATPS. An ATP-PDDA coacervate containing rhodamine B was dispensed by manual pipetting into a DEX-PEG system (Figure 1). Confocal imaging showed distinct boundaries of the coacervate, DEX, and PEG phases with rhodamine B confined to the coacervate phase (Figure 1A and Movie 1). UV-VIS spectroscopic measurements revealed that the crowded microenvironment in the DEX phase enables long-term retention of the coacervate with minimal disintegration compared to solutions in MES buffer (Figure 1B). Less than 5 % of the total ATP molecules dissociated from the coacervate in the DEX phase over 24 hours.

Next, we prepared ATP-PDDA coacervates containing different food colorings (Figure S2) and patterned the individual coacervates in the DEX-PEG system (Figure 1C). The ATPPDDA coacervates retained their shape without mixing and sufficiently sequestered the food colorings in the DEX-PEG system over 48 hours (Figure S3). The data are agreed well with the recent report,[31] claiming that the presence of molecular crowders such as PEG and DEX can assist the encapsulation of molecules in RNA-peptide coacervates. The results demonstrate that multiple ATP-PDDA coacervates can be spatially patterned and structurally maintained without rapid disintegration in the DEX-PEG system.

In contrast to aqueous multiphase systems that solely rely on immiscibility,[32] the individual coacervate phases in this system can be separately manipulated using pH, ionic strength, and constituent polymer concentrations.[33] We confirmed selective disintegration of the coacervates by increasing ionic strength or lowering pH (Figure S4). The ionic strength-driven release of compartmentalized biomolecules would be less harsh and a more versatile approach compared to pH change. We hypothesized that ion addition can functionally mimic "second messenger" signaling to trigger reactions. More specifically, by increasing the ionic strength, the ions triggered the release of encapsulated substances through selective disintegration of the coacervates while maintaining the DEX-PEG boundary (Figure S5 and Movie 2). The ATPPDDA coacervates gradually swelled over 5 min and completely dissociated in 15 min when exposed to 200 mM NaCl (Figure S5A–C). The food colorings were completely mixed while the DEX phase remained intact in the PEG phase for at least

1200 min (Figure S5D). The results demonstrate that the salt-induced regulation of the phase dynamics is potentially useful to initiate reactions.

Two-enzyme cascade reaction in the ATP-PDDA – DEX – PEG system

Membrane-less organelles facilitate metabolic cascade reactions[34] and signal transduction[35] by selective partitioning that sequesters certain biomolecules while allowing others to transit relatively freely between phases and by reversible phase separation. Similar to membraneless-organelles in cells, our system is a membrane-free platform where small molecules like nutrients can diffuse out through the boundaries while macromolecules are spatially sequestered.

To articulate this advantage, we demonstrated an enzymatic cascade reaction that starts with glucose oxidase (GOx) oxidizing glucose to produce hydrogen peroxide and ends with horseradish peroxidase (HRP) oxidizing substrates (Scheme 1A and Figure S3). This cascade reaction has commonly been adopted as a cell signaling model in compartmentalized systems.[36, 37] A single ATP-PDDA coacervate containing Amplex Red (HRP substrate) and HRP was dispensed into a DEX phase containing GOx, and this DEX phase was further surrounded by a PEG phase that contained β-glucose. The fluorescent signal from the ATP-PDDA coacervate was observed only when all essential components for the reaction were present in the system (Figure S6). FITC-labeled GOx showed that GOx was initially partitioned at the coacervate-DEX interface and gradually diffused into the coacervate phase over time (Figure S7). Multi-compartmentalization also enables the conduction of multiple reactions in defined spatial locations. In this context, we prepared three different substrates (ABTS, DAB, and oPD) together with HRP in different membraneless compartments (Scheme 1B). In the presence of glucose, colorimetric signals were observed. However, in the absence of glucose, no such signal was detected (Figure 2A and B). Additionally, no visible change was detected in the control coacervates. Interestingly, when we isolated HRP and DAB into separate compartments away from each droplet, no colorimetric change was observed over the course of our 60 minutes experiments due to insufficient time for DAB to diffusion from its droplet to the HRP-compartmentalized droplet (Figure 2C). In order to activate HRP substrates, HRP and its substrates need to be in close proximity to each other. The results confirm that the spatial control of components is essential to perform enzyme-mediated cascade reactions.[38–40]

Absorbance measurements highlight the effect of compartmentalization during the reaction (Figure 3). Interestingly, when the sequestered enzymes and substrates were released in the presence of 200 mM NaCl, the absorbance of the catalyzed products drastically dropped due to rapid diffusion of the substrate and product (Figure 3A–C). Since droplet size has been shown to affect the reaction rate,[41–43] we changed the volume of coacervate droplets while maintaining total amount of encapsulate HRP the same (Table S2). In addition to fixing the total mass of HRP in the coacervate droplet, we distributed DAB and GOx outside the coacervate in the DEX phase to maintain total amounts of DAB and GOx constant even. The results show that DAB distributed in the DEX droplet diffuses into the coacervate droplet and precipitates through HRP-mediated catalysis. The stark color contrast between the inside and outside of the coacervate droplet after the reaction illustrates robust

compartmentalization of HRP in the coacervate droplet (Figure S8). However, we found no significant difference in the production rate of DAB when normalized by the droplet volume (data not shown). Given the relatively constant and small surface-to-volume ratio among the droplets (Table S2), we speculate that the coacervate droplets in our experiments are all in the larger size regime making it difficult to observe significant size-mediated effect.

Altogether, these results illustrate that our system allows flexible manipulation of coacervate droplets formed within a DEX-PEG ATPS to regulate enzymatic reactions through membrane-less compartmentalization.

DEX degradation by dextranase is accelerated by sequestering the enzyme in an adjacent phase

An interesting feature of the nucleolus, a prominent membrane-less organelle, is that the enzymatic machinery is often sequestered in a separate phase adjacent to the phase in which their biopolymer substrates are present in higher concentrations. For example, RNA polymerase I is exclusively sequestered in the nucleolus where the DNA concentration is relatively low compared to the nucleoplasm.[44] It would be more intuitive for enzymes and substrates to be co-localized to accelerate reactions. What might be the effect of such separation of enzyme and substrate?

Hypothesizing that there is a difference during the reaction process when the substrate concentration is high such as in the cases where the substrate comprises one of the phase forming polymers, we tested the effect of sequestering dextranase away from its substrate DEX. We prepared RITC-labeled dextranase and compared time-lapse DEX degradation when dextranase is sequestered in coacervate droplets away from DEX macromolecules or released directly into the DEX phase (Figure 4). As expected, negligible DEX degradation was observed in the complete absence of dextranase (Figure 4C). Interestingly, however, RITC-dextranase compartmentalized in the ATP-PDDA coacervate adjacent to but away from the DEX phase degraded DEX faster than when the enzyme was distributed directly into the DEX phase (Figure 4A and B). The DEX degradation showed a distinct profile depending on the distribution of dextranase (Figure 4D). We note that the coacervate size was constant in the absence of NaCl over 24 hours and the DEX degradation was repeatable when new DEX droplets were supplied after complete degradation of the original DEX (data not shown).

Reduced substrate inhibition of dextranase when compartmentalized by ATP-PDDA coacervates

To understand the underlying mechanism, we performed a conventional dextranase assay in bulk conditions without the PEG phase (Figure 5). Given that the dextranase used in our manuscript is an endo-dextranase, we note that the dextranase product is also dextran of a smaller molecular weight and is hence also a substrate analogue. Dextranase showed negligible difference in enzyme activity regardless of the presence or absence of 150 mM NaCl (Figure 5A). Interestingly, despite the same amount of dextranase, significantly higher activity in the coacervate-compartmentalized dextranase was observed compared to the DEX-compartmentalized dextranase. Kinetics analysis suggests that substrate inhibition is

occurring when the dextranase is exposed directly to the DEX phase (Figure 5B). Importantly, there is no significant difference in reaction velocity between the compartmentalized and released conditions in the low concentration regime where no substrate inhibition is observed (up until 1% DEX). It is only in regimes where substrate inhibition is observed (2%, 3%, 8%, and 10% DEX) that compartmentalization provides a reaction velocity advantage. This further supports the notion that compartmentalization enhances reactions by alleviating substrate inhibition.

The another interesting feature of the results include the relatively steep drop in reaction velocity above DEX 2% that is difficult to explain simply by substrate inhibition alone, and the drastic reduction in reaction velocity of even the compartmentalized condition at 20% DEX. Given high molecular weight of DEX macromolecules (~500 $kg \cdot mol^{-1}$), we compared the viscosities of the different DEX formulations (Figure S9). We found drastically higher viscosity at 20% DEX (~200 mPa·s) compared to 1% DEX (1.5 mPa·s) (Figure S9A and B). This may explain the overall slow reaction velocities at 20% DEX. Although the viscosities of 2% – 10% DEX solutions also increased (2~20 mPa·s), perhaps not to the extent that all the reaction velocity decrease can be ascribed to higher viscosity. We additionally estimated the viscosity of the coacervate phase from the measured relative viscosity (Figure S9C) and the value was comparable to that of 15% DEX (~100 mPa·s). Thus, viscosity decrease is not the reason for reaction acceleration in the compartmentalized system. Overall, we suggest that viscosity may play some role in the observed reaction velocity changes but not an overwhelming role.

Dextranase is an industrial enzyme used to reduce viscosity in sugar mills.[45] Although the activity drop of dextranase at a high dextran concentration has been reported,[46] this is, as far as we know, the first demonstration of the acceleration of dextranase reactions by enzyme compartmentalization from substrate inhibition. Our findings therefore may have some industrial relevance in sugar processing efficiency. More importantly, the results suggest mitigation of reaction inhibition by sequestration of enzymes away from the phase where its substrate and substrate analogues dominate as a potential mechanism by which membraneless organelles can accelerate bioreactions.

Recent studies have revealed that membrane-less organelles composed of protein-protein[47–49] or protein-nucleic acid[50–52] complexes are prevalent in the nucleus and cytoplasm and linked to protein aggregation-related diseases,[53–55] cancer,[56] and stress response.[57, 58] In the nucleolus, for example, membrane-less compartmentalization is known to concentrate RNAP I and boost the transcription rate.[59] A recent study demonstrates upregulation of hyperphospholyration of RNAP II upon membrane-less compartmentalization through LLPS of kinase proteins in nuclear speckels.[60] Such reaction acceleration by enzyme sequestration is traditionally assumed to be due to co-localization and better proximity between the enzyme and its reaction partners.[61–63] Additionally, sequestration of biomolecules away from its reaction partners is generally considered as a way to slow reactions down. For example, nucleolar detention has been reported as a regulatory mechanism cells under stress adopt to sequester reaction intermediates to slow metabolic reactions down.[64, 65]

Here, we show that sequestration of enzymes to a membrane-less compartment away from substrates can unexpectedly accelerate reactions by alleviating substrate inhibition in cases where the substrate concentration is high. As segregated compartmentalization of enzymes and their reaction partners is not uncommon in the cells, reaction acceleration by alleviation of inhibition by substrates and substrate-mimetics may be physiologically relevant. While this paper focuses on man-made polymer systems, we believe the insights can inspire additional analysis of nucleic acid-protein systems that are more directly related to epigenetics[66–68] as well as neurodegenerative diseases and cancer.[69]

4. Conclusions

We report the formation of multiple stable membrane-less compartments comprised of ATP-PDDA coacervation and DEX-PEG ATPS. The system recreates aspects of membraneless organelles using readily-available chemicals and materials to allow functional studies of the biochemical implications of such compartmentalization. Because coacervate droplets and DEXPEG ATPS have very distinct phase forming responses to ionic strength, pH, and dextranase, this combination allowed orthogonal manipulation of the different phases. For example, enzymes and substrates sub-compartmentalized within the coacervates could be released into the DEX compartment upon coacervate degradation by increased ionic strength or pH change. Alternatively, compartmentalization of dextranase in the coacervate droplets, even as the DEX phase was degraded by hydrolysis, enabled insight into unique ability of membraneless compartmentalization to reduce substrate inhibition.

Our robust membrane-free system recapitulates aspects of physiologically relevant membrane-less compartmentalization and sheds light on a previously overlooked mechanism of reaction acceleration by reducing reaction inhibition by substrate and substrate-analogues. While this manuscript focuses on dextranase and substrate inhibition caused by DEX, it may be interesting to interrogate other enzymatic reactions that demonstrate substrate inhibition.

Supplementary Material

Refer to Web version on PubMed Central for supplementary material.

Acknowledgements

We thank the NIH (R01 GM123517 and CA 196018) and NSF (CBET 0939511) for funding.

Abbreviation

ATPS	aqueous two phase system
LLPS	liquid-liquid phase separation
ATP	adenosine triphosphate
PDDA	poly(diallyldimethylammonium chloride)
DEX	dextran

PEG	polyethylene glycol
HRP	horseradish peroxidase
GOx	glucose oxidase
FITC	fluorescein isothiocyanate
RITC	rhodamine B isothiocyanate
ABTS	2,2’-azino-bis(3-ethylbenzothiazoline-6-sulfonic acid) diammonium salt
DAB	3,3’-diaminobenzidine
oPD	o-phenylenediamine
MES	2-(N-morpholino)ethanesulfonic acid
MOPS	3-morpholinopropane-1-sulfonic acid
NaOH	sodium hydroxide
HCl	hydrochloric acid
DNA	deoxyribonucleic acid
RNA	ribonucleic acid
RNAP	RNA polymerase

References

1. Marguet M; Bonduelle C and Lecommandoux S, Multicompartmentalized Polymeric Systems: Towards Biomimetic Cellular Structure and Function. Chem. Soc. Rev 2013, 42, 512–529. [PubMed: 23073077]
2. Li M; Huang X; Tang TD and Mann S, Synthetic Cellularity Based on Non-Lipid Micro-Compartments and Protocell Models. Curr. Opin. Chem. Biol 2014, 22, 1–11. [PubMed: 24952153]
3. Schmitt C; Lippert AH; Bonakdar N; Sandoghdar V and Voll LM, Compartmentalization and Transport in Synthetic Vesicles. Front. Bioeng. Biotechnol 2016, 4, 19. [PubMed: 26973834]
4. Buddingh’ BC and van Hest JC, Artificial Cells: Synthetic Compartments with Life-like Functionality and Adaptivity. Acc. Chem. Res 2017, 50, 769–777. [PubMed: 28094501]
5. Brangwynne CP; Eckmann CR; Courson DS; Rybarska A; Hoege C; Gharakhani J; Jülicher F and Hyman AA, Germline P Granules Are Liquid Droplets That Localize by Controlled Dissolution/ Condensation. Science 2009, 324, 1729–1732. [PubMed: 19460965]
6. Li X-H; Chavali PL; Pancsa R; Chavali S and Babu MM, Function and Regulation of Phase-Separated Biological Condensates. Biochemistry 2018, 57, 2452–2461. [PubMed: 29392932]
7. Boeynaems S; Alberti S; Fawzi NL; Mittag T; Polymenidou M; Rousseau F; Schymkowitz J; Shorter J; Wolozin B and Van Den Bosch L, Protein Phase Separation: A New Phase in Cell Biology. Trends Cell Biol. 2018, doi: 10.1016/j.tcb.2018.1002.1004.
8. Bergeron-Sandoval L-P; Safaee N and Michnick SW, Mechanisms and Consequences of Macromolecular Phase Separation. Cell 2016, 165, 1067–1079. [PubMed: 27203111]
9. Delarue M; Brittingham G; Pfeffer S; Surovtsev I; Pinglay S; Kennedy K; Schaffer M; Gutierrez J; Sang D and Poterewicz G, mTORC1 Controls Phase Separation and the Biophysical Properties of the Cytoplasm by Tuning Crowding. Cell 2018, doi: 10.1016/j.cell.2018.1005.1042.

10. Woodruff JB; Gomes BF; Widlund PO; Mahamid J; Honigmann A and Hyman AA, The Centrosome Is a Selective Condensate That Nucleates Microtubules by Concentrating Tubulin. Cell 2017, 169, 1066–1077. e1010. [PubMed: 28575670]
11. Su X; Ditlev JA; Hui E; Xing W; Banjade S; Okrut J; King DS; Taunton J; Rosen MK and Vale RD, Phase Separation of Signaling Molecules Promotes T Cell Receptor Signal Transduction. Science 2016, 352, 595–599. [PubMed: 27056844]
12. Banani SF; Lee HO; Hyman AA and Rosen MK, Biomolecular Condensates: Organizers of Cellular Biochemistry. Nat. Rev. Mol. Cell Biol. 2017, 18, 285–298. [PubMed: 28225081]
13. Strulson CA; Molden RC; Keating CD and Bevilacqua PC, RNA Catalysis Through Compartmentalization. Nat. Chem 2012, 4, 941–946. [PubMed: 23089870]
14. Decker CJ and Parker R, P-bodies and Stress Granules: Possible Roles in The Control of Translation and mRNA Degradation. Cold Spring Harb Perspect Biol. 2012, 4, a012286. [PubMed: 22763747]
15. Buchan JR, mRNP Granules: Assembly, Function, and Connections with Disease. RNA Biol. 2014, 11, 1019–1030. [PubMed: 25531407]
16. Rabouille C and Alberti S, Cell Adaptation upon Stress: The Emerging Role of Membrane-Less Compartments. Curr Opin Cell Biol. 2017, 47, 34–42. [PubMed: 28342303]
17. Aguilera-Gomez A and Rabouille C, Membrane-Bound Organelles Versus Membrane-Less Compartments and Their Control of Anabolic Pathways in Drosophila. Dev. Biol 2017, 428, 310–317. [PubMed: 28377034]
18. Koga S; Williams DS; Perriman AW and Mann S, Peptide–Nucleotide Microdroplets as A Step towards A Membrane-Free Protocell Model. Nat. Chem 2011, 3, 720–724. [PubMed: 21860462]
19. Williams DS; Koga S; Hak CRC; Majrekar A; Patil AJ; Perriman AW and Mann S, Polymer/Nucleotide Droplets as Bio-Inspired Functional Micro-Compartments. Soft Matter 2012, 8, 6004–6014.
20. Albertsson P-Å, Partition of Cell Particles and Macromolecules. 3rd ed.; Wiley New York: 1986.
21. Kojima T and Takayama S, Patchy Surfaces Stabilize Dextran–Polyethylene Glycol Aqueous Two-Phase System Liquid Patterns. Langmuir 2013, 29, 5508–5514. [PubMed: 23581424]
22. Kojima T and Takayama S, Microanalysis Using Surface Modification and Biphasic Droplets. Polym. J 2018, doi:10.1038/s41428-41018-40050-x.
23. Reed MC; Lieb A and Nijhout HF, The Biological Significance of Substrate Inhibition: A Mechanism with Diverse Functions. Bioessays 2010, 32, 422–429. [PubMed: 20414900]
24. Olson MO; Dundr M and Szebeni A, The Nucleolus: An Old Factory with Unexpected Capabilities. Trends Cell Biol. 2000, 10, 189–196. [PubMed: 10754561]
25. Berry J; Weber SC; Vaidya N; Haataja M and Brangwynne CP, RNA Transcription Modulates Phase Transition-Driven Nuclear Body Assembly. Proc. Natl. Acad. Sci. U.S.A. 2015, 112, E5237–E5245. [PubMed: 26351690]
26. Williams DS; Patil AJ and Mann S, Spontaneous Structuration in Coacervate:Based Protocells by Polyoxometalate:Mediated Membrane Assembly. Small 2014, 10, 1830–1840. [PubMed: 24515342]
27. Armstrong JP; Olof SN; Jakimowicz MD; Hollander AP; Mann S; Davis SA; Miles MJ; Patil AJ and Perriman AW, Cell Paintballing Using Optically Targeted Coacervate Microdroplets. Chem. Sci 2015, 6, 6106–6111. [PubMed: 30090225]
28. Kojima T and Takayama S, Microscale Determination of Aqueous Two Phase System Binodals by Droplet Dehydration in Oil. Anal. Chem 2013, 85, 5213–5218. [PubMed: 23614634]
29. Elbaum-Garfinkle S; Kim Y; Szczepaniak K; Chen CC-H; Eckmann CR; Myong S and Brangwynne CP, The Disordered P Granule Protein LAF-1 Drives Phase Separation into Droplets with Tunable Viscosity and Dynamics. Proc. Natl. Acad. Sci. U.S.A. 2015, 112, 7189–7194. [PubMed: 26015579]
30. Milin AN and Deniz AA, Reentrant Phase Transitions and Non-Equilibrium Dynamics in Membraneless Organelles. Biochemistry 2018, 57, 2470–2477. [PubMed: 29569441]
31. Marianelli A; Miller B and Keating C, Impact of Macromolecular Crowding on RNA/Spermine Complex Coacervation and Oligonucleotide Compartmentalization. Soft Matter 2018, 14, 368–378. [PubMed: 29265152]

32. Torre P; Keating CD and Mansy SS, Multiphase Water-In-Oil Emulsion Droplets for Cell-Free Transcription–Translation. Langmuir 2014, 30, 5695–5699. [PubMed: 24810327]
33. Aumiller WM, Jr and Keating CD, Phosphorylation-Mediated RNA/Peptide Complex Coacervation as a Model for Intracellular Liquid Organelles. Nat. Chem 2016, 8, 129–137. [PubMed: 26791895]
34. Jørgensen K; Rasmussen AV; Morant M; Nielsen AH; Bjarnholt N; Zagrobelny M; Bak S and Møller BL, Metabolon Formation and Metabolic Channeling in the Biosynthesis of Plant Natural Products. Curr. Opin. Plant Biol. 2005, 8, 280–291. [PubMed: 15860425]
35. Wu H, Higher-Order Assemblies in a New Paradigm of Signal Transduction. Cell 2013, 153, 287–292. [PubMed: 23582320]
36. Aumiller WM, Jr; Davis BW; Hashemian N; Maranas C; Armaou A and Keating CD, Coupled Enzyme Reactions Performed in Heterogeneous Reaction Media: Experiments and Modeling for Glucose Oxidase and Horseradish Peroxidase in A PEG/Citrate Aqueous Two-phase System. J. Phys. Chem. B 2014, 118, 2506–2517. [PubMed: 24517887]
37. Tan H; Guo S; Dinh N-D; Luo R; Jin L and Chen C-H, Heterogeneous Multi-Compartmental Hydrogel Particles as Synthetic Cells for Incompatible Tandem Reactions. Nat. Commun 2017, 8, 663. [PubMed: 28939810]
38. Vriezema DM; Garcia PM; Sancho Oltra N; Hatzakis NS; Kuiper SM; Nolte RJ; Rowan AE and van Hest J, Positional Assembly of Enzymes in Polymersome Nanoreactors for Cascade Reactions. Angew. Chem 2007, 119, 7522–7526.
39. Van Albada SB and Ten Wolde PR, Enzyme Localization Can Drastically Affect Signal Amplification in Signal Transduction Pathways. PLOS Comput. Biol 2007, 3, e195.
40. Liu X; Formanek P; Voit B and Appelhans D, Functional Cellular Mimics for the Spatiotemporal Control of Multiple Enzymatic Cascade Reactions. Angew. Chem 2017, 129, 16451–16456.
41. Xue F; Zhang Y; Zhang F; Ren X and Yang H, Tuning the Interfacial Activity of Mesoporous Silicas for Biphasic Interface Catalysis Reactions. ACS applied materials & interfaces 2017, 9, 8403–8412. [PubMed: 28195458]
42. Zhang M; Wei L; Chen H; Du Z; Binks BP and Yang H, Compartmentalized Droplets for Continuous Flow Liquid–Liquid Interface Catalysis. J. Am. Chem. Soc 2016, 138, 10173–10183. [PubMed: 27429173]
43. Zhang M; Ettelaie R; Yan T; Zhang S; Cheng F; Binks BP and Yang H, Ionic Liquid Droplet Microreactor for Catalysis Reactions Not at Equilibrium. J. Am. Chem. Soc 2017, 139, 17387–17396. [PubMed: 29099180]
44. Sirri V; Urcuqui-Inchima S; Roussel P and Hernandez-Verdun D, Nucleolus: The Fascinating Nuclear Body. Histochem. Cell Biol 2008, 129, 13–31. [PubMed: 18046571]
45. Jiménez ER, Dextranase in Sugar Industry: A Review. Sugar Tech 2009, 11, 124–134.
46. Pleszczyńska M; Szczodrak J; Rogalski J and Fiedurek J, Hydrolysis of Dextran by Penicillium Notatum Dextranase and Identification of Final Digestion Products. Mycological Research 1997, 101, 69–72.
47. Li P; Banjade S; Cheng H-C; Kim S; Chen B; Guo L; Llaguno M; Hollingsworth JV; King DS and Banani SF, Phase Transitions in the Assembly of Multivalent Signalling Proteins. Nature 2012, 483, 336–340. [PubMed: 22398450]
48. Nott TJ; Petsalaki E; Farber P; Jervis D; Fussner E; Plochowietz A; Craggs TD; Bazett-Jones DP; Pawson T and Forman-Kay JD, Phase Transition of a Disordered Nuage Protein Generates Environmentally Responsive Membraneless Organelles. Mol. Cell 2015, 57, 936–947. [PubMed: 25747659]
49. Lin Y; Protter DS; Rosen MK and Parker R, Formation and Maturation of Phase-Separated Liquid Droplets by Rna-Binding Proteins. Mol. Cell 2015, 60, 208–219. [PubMed: 26412307]
50. Brangwynne CP; Mitchison TJ and Hyman AA, Active Liquid-like Behavior of Nucleoli Determines Their Size and Shape in Xenopus Laevis Oocytes. Proc. Natl. Acad. Sci. U.S.A. 2011, 108, 4334–4339. [PubMed: 21368180]
51. Molliex A; Temirov J; Lee J; Coughlin M; Kanagaraj AP; Kim HJ; Mittag T and Taylor JP, Phase Separation by Low Complexity Domains Promotes Stress Granule Assembly and Drives Pathological Fibrillization. Cell 2015, 163, 123–133. [PubMed: 26406374]

52. Feric M; Vaidya N; Harmon TS; Mitrea DM; Zhu L; Richardson TM; Kriwacki RW; Pappu RV and Brangwynne CP, Coexisting Liquid Phases Underlie Nucleolar Subcompartments. Cell 2016, 165, 1686–1697. [PubMed: 27212236]
53. Patel A; Lee HO; Jawerth L; Maharana S; Jahnel M; Hein MY; Stoynov S; Mahamid J; Saha S and Franzmann TM, A Liquid-To-Solid Phase Transition of the ALS Protein Fus Accelerated by Disease Mutation. Cell 2015, 162, 1066–1077. [PubMed: 26317470]
54. Shin Y and Brangwynne CP, Liquid Phase Condensation in Cell Physiology and Disease. Science 2017, 357, eaaf4382. [PubMed: 28935776]
55. Jain A and Vale RD, RNA Phase Transitions in Repeat Expansion Disorders. Nature 2017, 546, 243–247. [PubMed: 28562589]
56. Marzahn MR; Marada S; Lee J; Nourse A; Kenrick S; Zhao H; Ben-Nissan G; Kolaitis RM; Peters JL and Pounds S, Higher:Order Oligomerization Promotes Localization of Spop to Liquid Nuclear Speckles. EMBO J. 2016, e201593169.
57. Riback JA; Katanski CD; Kear-Scott JL; Pilipenko EV; Rojek AE; Sosnick TRand Drummond, D. A., Stress-Triggered Phase Separation Is an Adaptive, Evolutionarily Tuned Response. Cell 2017, 168, 1028–1040. e1019. [PubMed: 28283059]
58. Franzmann TM; Jahnel M; Pozniakovsky A; Mahamid J; Holehouse AS; Nüske E; Richter D; Baumeister W; Grill SW and Pappu RV, Phase Separation of a Yeast Prion Protein Promotes Cellular Fitness. Science 2018, 359, eaao5654. [PubMed: 29301985]
59. Yu F, High Concentration of RNA Polymerase I Is Responsible for the High Rate of Nucleolar Transcription. Biochem. J 1980, 188, 381–385. [PubMed: 6156675]
60. Lu H; Yu D; Hansen AS; Ganguly S; Liu R; Heckert A; Darzacq X and Zhou Q, Phase-Separation Mechanism for C-Terminal Hyperphosphorylation of RNA Polymerase II. Nature 2018, 558, 318–323. [PubMed: 29849146]
61. Li J; Nayak S and Mrksich M, Rate Enhancement of an Interfacial Biochemical Reaction Through Localization of Substrate and Enzyme by an Adaptor Domain. J. Phys. Chem. B 2010, 114, 15113–15118. [PubMed: 21047083]
62. Castellana M; Wilson MZ; Xu Y; Joshi P; Cristea IM; Rabinowitz JD; Gitai Z and Wingreen NS, Enzyme Clustering Accelerates Processing of Intermediates Through Metabolic Channeling. Nat. Biotechnol 2014, 32, 1011–1018. [PubMed: 25262299]
63. Davis BW; Aumiller WM, Jr; Hashemian N; An S; Armaou A and Keating CD, Colocalization and Sequential Enzyme Activity in Aqueous Biphasic Systems: Experiments and Modeling. Biophys. J 2015, 109, 2182–2194. [PubMed: 26588576]
64. Audas TE; Jacob MD and Lee S, Immobilization of Proteins in The Nucleolus by Ribosomal Intergenic Spacer Noncoding RNA. Mol. Cell 2012, 45, 147–157. [PubMed: 22284675]
65. Audas TE; Jacob MD and Lee S, The Nucleolar Detention Pathway: A Cellular Strategy for Regulating Molecular Networks. Cell Cycle 2012, 11, 2059–2062. [PubMed: 22580471]
66. Monahan Z; Ryan VH; Janke AM; Burke KA; Rhoads SN; Zerze GH; O'Meally R; Dignon GL; Conicella AE and Zheng W, Phosphorylation of the FUS Low:Complexity Domain Disrupts Phase Separation, Aggregation, and Toxicity. EMBO J. 2017, e201696394.
67. Larson AG; Elnatan D; Keenen MM; Trnka MJ; Johnston JB; Burlingame AL; Agard DA; Redding S and Narlikar GJ, Liquid Droplet Formation by HP1α Suggests a Role for Phase Separation in Heterochromatin. Nature 2017, 547, 236–240. [PubMed: 28636604]
68. Hofweber M; Hutten S; Bourgeois B; Spreitzer E; Niedner-Boblenz A; Schifferer M; Ruepp M-D; Simons M; Niessing D and Madl T, Phase Separation of FUS Is Suppressed by Its Nuclear Import Receptor and Arginine Methylation. Cell 2018, 173, 706–719. e713. [PubMed: 29677514]
69. Aguzzi A and Altmeyer M, Phase Separation: Linking Cellular Compartmentalization to Disease. Trends Cell Biol. 2016, 26, 547–558. [PubMed: 27051975]

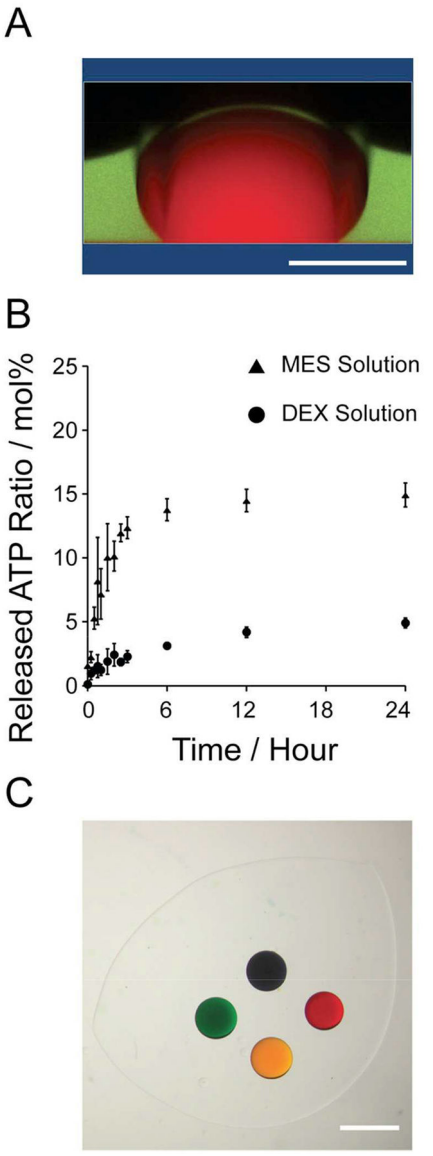

Figure 1.

Membrane-less compartmentalization using ATP-PDDA coacervates in a 10% DEX – 10% PEG system. (A) Reconstructed Z-stack image of a rhodamine B-encapuslating ATP-PDDA droplet (red) resuspended in a DEX droplet (green) in the PEG phase (black). Red: rhodamine B and green: FITC-DEX. (B) Time-lapse release of ATP from the coacervate quantified by UV-VIS spectroscopy measurement in MES (closed triangle) or the DEX (closed circle) solutions over 24 hours. The released ATP was normalized by the total ATP in the coacervate (mol%). The total ATP was obtained by complete coacervate dissociation by NaCl addition. (C) A brightfield image of the ATP-PDDA coacervates encapsulating food colorings (blue, red, yellow, and green) in the DEX-PEG ATPS. Scale bar (A) 500 μm and (C) 1 mm.

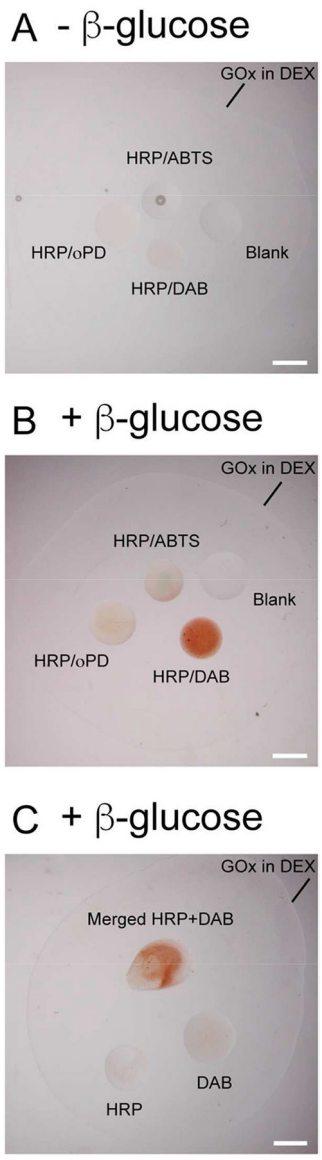

Figure 2.

Enzymatic cascade reactions across membrane-less compartments using GOx and HRP in the DEX-PEG ATPS. A GOx-suspended DEX droplet was submerged by a PEG solution. HRP-ABTS-laden coacervate (top), HRP-oPD-laden coacervate (left), HRP-DAB-laden coacervate (bottom), and blank coacervate (right) were spotted in the DEX deroplet. The images were taken (A) in the absence and (B) in the presence of 1 mM β-glucose at t = 60 min, respectively. (C) The DAB-laden (bottom left) and HRP-laden (bottom right) coacervates were either isolated or overlaid (top) in the presence of 1 mM β-glucose. The image was taken at t = 60 min. Scale bar 1 mm.

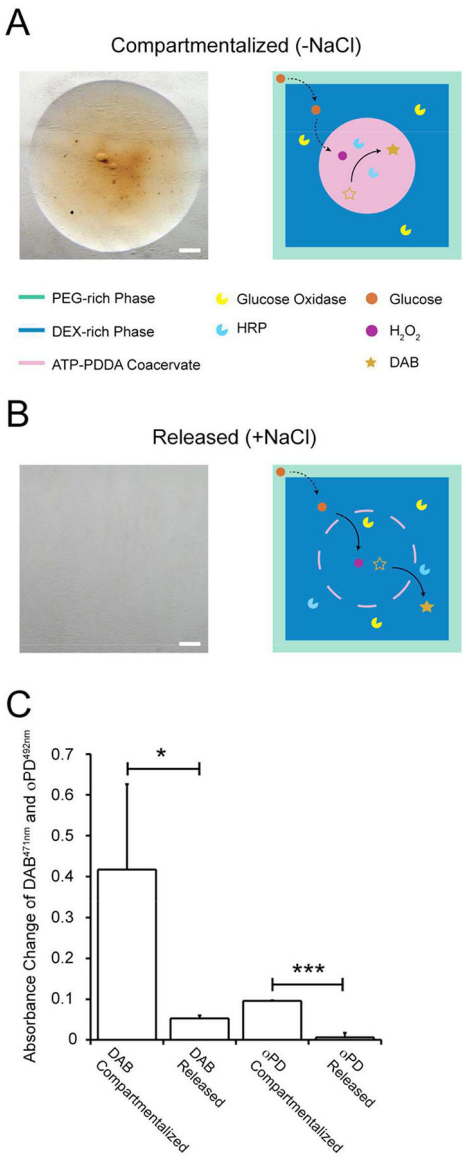

Figure 3.

A colorimetric assay of the cascade reaction under compartmentalized and released conditions. (A) The compartmentalized HRP-DAB in the absence of 200 mM NaCl at t = 90 min. (B) The released HRP-DAB in the presence of 200 mM NaCl at t = 90 min. (C) Absorbance change of DAB (l = 471 nm) and oPD (l = 492 nm) using compartmentalized or released HRP-DAB or HRP-oPD. Scale bar 1 mm. The bar indicates individual pairwise differences: * $p < 0.05$ and *** $p < 0.01$.

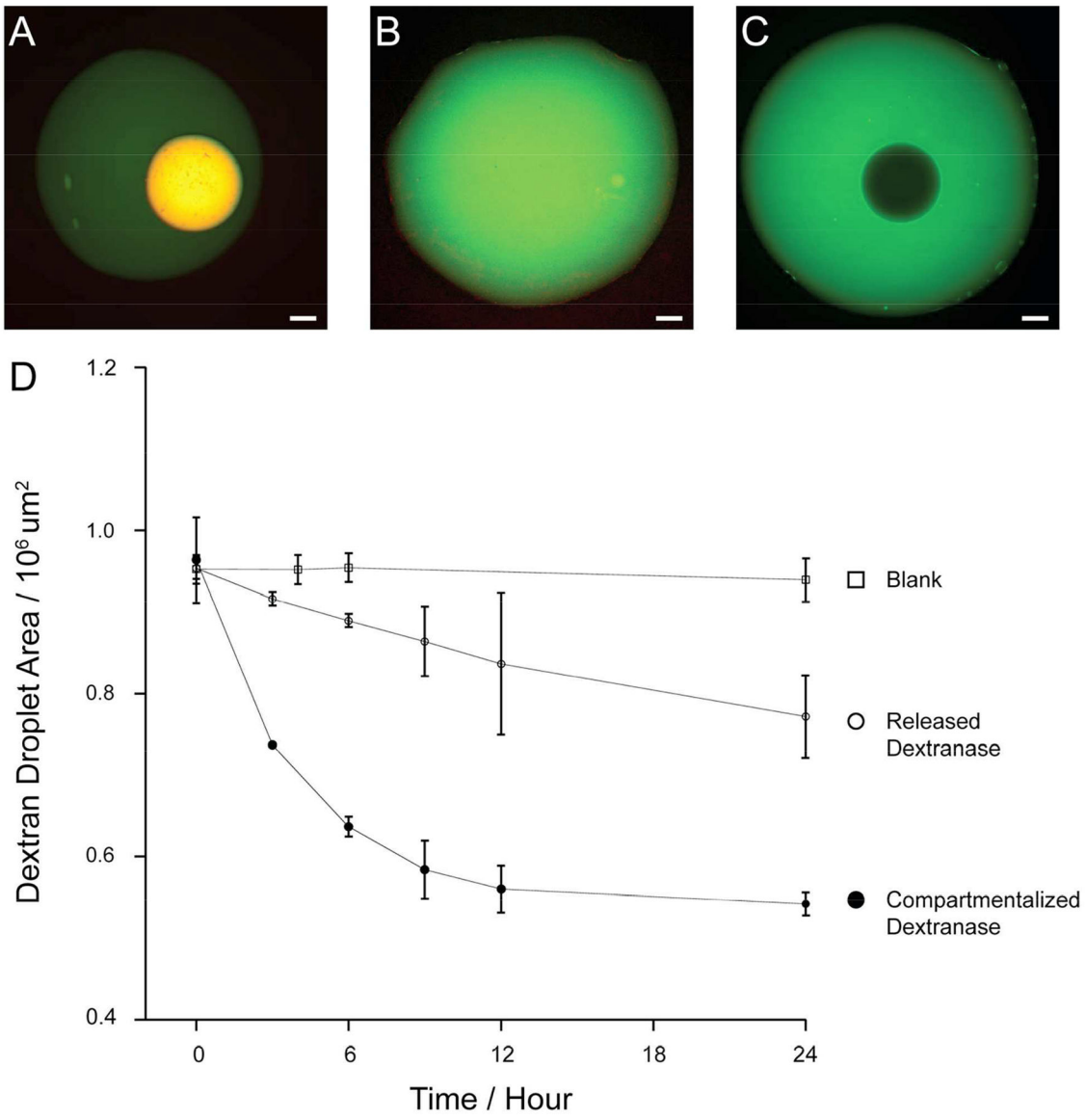

Figure 4.

A dextran degradation assay comparing compartmentalized and released dextranase. (A) Dextranase was compartmentalized in ATP-PDDA coacervate droplets in a DEX-PEG system. (B) Dextranase was released from the coacervate phase upon disintegration of the coacervate phase triggered by the addition of 150 mM NaCl. (C) A blank ATP-PDDA coacervate was used as a control condition. The images were taken at t = 24 hrs. Green: FITC-DEX and red: RITC-dextranase. Scale bar 100 μm. (D) The area shrinkage of DEX droplets was analyzed over 24 hours.

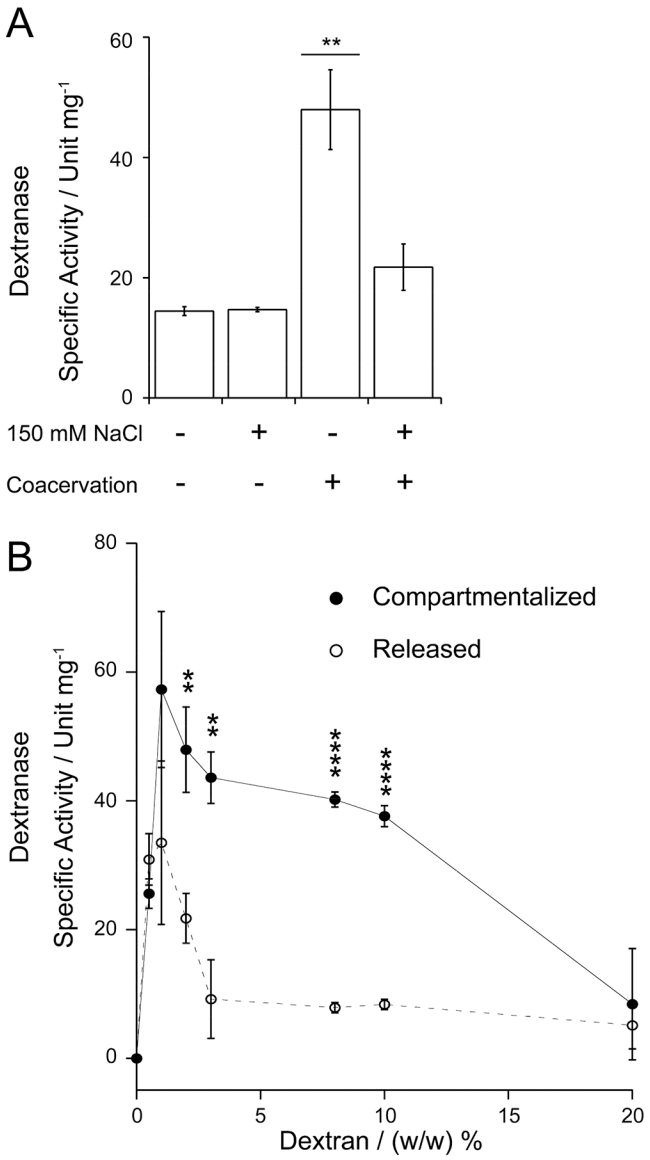

Figure 5.

A bulk dextranase assay comparing compartmentalized and released dextranase. (A) The specific activity of bulk dextranase in a 2 % (w/w) DEX solution was quantified at 24 °C using compartmentalized or released dextranase in the ATP-PDDA coacervates. Free-floating dextranase with a similar amount of mass (2 μg) in the presence and absence of 150 mM NaCl was used as control conditions. The bar indicates pairwise comparison to all others in that group: ** $p < 0.01$. (B) The specific activity of compartmentalized and released dextranase at 24 °C was measured as a function of the DEX concentration. The astarisk indicates pairwise comparison at each DEX concentration: ** $p < 0.01$, **** $p < 0.0001$.

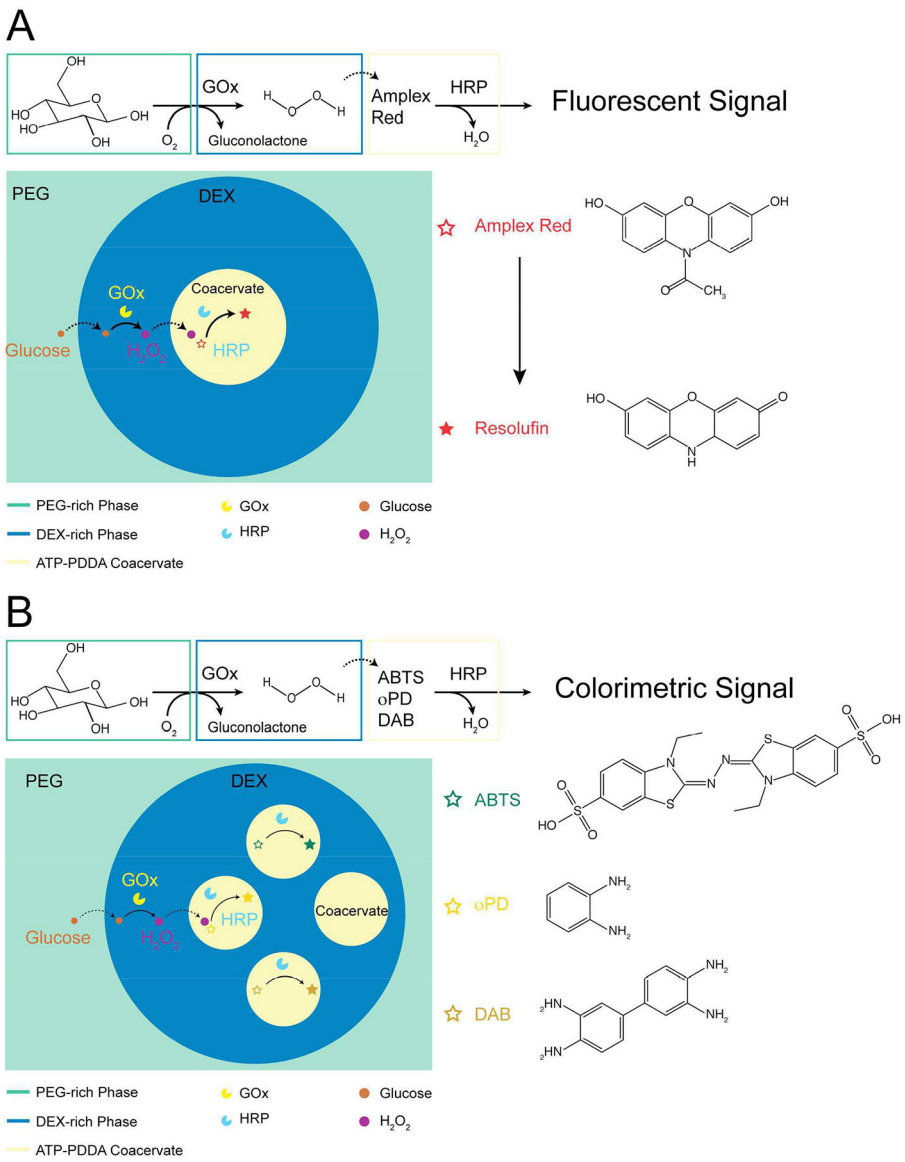

Scheme 1.

A schematic illustration of cascade reactions in the multicompartment system. (A) Single coacervate encapsulating HRP and Amplex Red in the DEX-PEG ATPS. (B) Multiple coacervates encapsulating HRP and ABTS, oPD or DAB in the DEX-PEG ATPS.